Journal of Power Sources 196 (2011) 8435–8443

Contents lists available at ScienceDirect

Journal of Power Sources

journal homepage: www.elsevier.com/locate/jpowsour

Glass-containing composite cathode contact materials for solid oxide fuel cells

Michael C. Tucker[a,*], Lei Cheng[a], Lutgard C. DeJonghe[b]

[a] Environmental Energy Technology Division, Lawrence Berkeley National Laboratory, 1 Cyclotron Rd Berkeley, CA 94720, United States
[b] Materials Sciences Division, Lawrence Berkeley National Laboratory, 1 Cyclotron Rd Berkeley, CA 94720, United States

ARTICLE INFO

Article history:
Received 15 April 2011
Received in revised form 13 May 2011
Accepted 19 May 2011
Available online 12 June 2011

Keywords:
Fuel cell
SOFC
CCM
Cathode contact
ASR

ABSTRACT

The feasibility of adding glass to conventional SOFC cathode contact materials in order to improve bonding to adjacent materials in the cell stack is assessed. A variety of candidate glass compositions are added to LSM and SSC. The important properties of the resulting composites, including conductivity, sintering behavior, coefficient of thermal expansion, and adhesion to LSCF and $Mn_{1.5}Co_{1.5}O_4$-coated 441 stainless steel are used as screening parameters. Adhesion of LSM to LSCF improved from 3.9 to 5.3 MPa upon addition of SCZ-8 glass. Adhesion of LSM to coated stainless steel improved from 1.8 to 3.9 MPa upon addition of Schott GM31107 glass. The most promising cathode contact material/glass composites are coated onto $Mn_{1.5}Co_{1.5}O_4$-coated 441 stainless steel substrates and subjected to area-specific resistance testing at 800 °C. In all cases, area-specific resistance is found to be in the range 2.5–7.5 mOhm cm^2 and therefore acceptable. Indeed, addition of glass is found to improve bonding of the cathode contact material layer without sacrificing acceptable conductivity.

1. Introduction

Assembly of solid oxide fuel cell (SOFC) stacks typically involves mechanically and electrically connecting a number of cells and interconnects in series. Connection of the cathode to the interconnect (or coating on the interconnect) is usually accomplished by compression of the stack using an external load frame, and is often aided by the use of a cathode contact material (CCM). The CCM is an electrically conductive material, and is applied as a paste or ink during stack assembly to form a continuous layer or discrete contact pads. The CCM provides electrical connection between the cathode and interconnect, and can also serve to improve in-plane conduction over the area of the cathode. Fig. 1 indicates placement of the CCM in the fuel cell stack. Often, the CCM is simply a thick layer of the electrocatalyst used in the cathode [1]. For example, a thin LSM–YSZ cathode layer optimized for electrochemical activity can be covered with a thick LSM–CCM layer optimized for gas transport and electrical conductivity. A significant limitation of this approach, however, is that most cathode compositions require firing at high temperature (>1100 °C) to achieve good sintering [2]. The use of ferritic stainless steel as the interconnect material limits the firing temperature to 1000 °C or lower. In practice, therefore, using a cathode catalyst CCM in conjunction with a stainless steel interconnect results in low CCM layer strength and minimal adhesion at the CCM/interconnect or CCM/cathode interface.

Efforts to decrease the required sintering temperature through doping [3] and control of the defect structure [3,4] have had some success. In the present work, we assess the merit of adding glass to the CCM in order to improve sintering and bonding without sacrificing acceptable conductivity of the resulting glass-ceramic composite.

2. Approach

The CCM composition must fulfill the following requirements:

- high electronic conductivity
- sintering/bonding at 1000 °C or lower
- good CTE match to other cell components
- mechanical strength within the CCM layer and at the interfaces to cathode and interconnect

Our approach is to fabricate composite mixtures of SOFC cathode material and glass. Glass compositions are widely used as seals for SOFCs, because they bond and wet to other SOFC materials at 1000 °C or below, producing mechanically robust seals [5,6]. The goal is to prepare a CCM composition that displays improved sintering and bonding via addition of glass, without sacrificing conductivity or long term stability of the resulting mixture.

Abbreviations: SOFC, solid oxide fuel cell; CCM, cathode contact material; ASR, area-specific resistance; CT, coefficient of thermal expansion; LSM, $La_{0.65}Sr_{0.3}Mn$ oxide; LSCF, $La_{0.6}Sr_{0.4}Co_{0.8}Fe_{0.2}$ oxide; SSC, $Sm_{0.5}Sr_{0.5}Co$ oxide; MCO, $Mn_{1.5}Co_{1.5}$ oxide; YSZ, Yttria-stabilized zirconia; XRD, X-ray diffraction; SEM, scanning electron microscopy; EDAX, energy dispersive analysis by X-rays.

* Corresponding author. Tel.: +1 510 486 5304; fax: +1 510 486 4881.
E-mail address: mctucker@lbl.gov (M.C. Tucker).

0378-7753/$ – see front matter © 2011 Elsevier B.V. All rights reserved.
doi:10.1016/j.jpowsour.2011.05.055

Table 1
Thermo-mechanical properties of various glasses.

Glass identifier	Manufacturer designation	CTE (ppm K^{-1})	Softening point (°C)
SPG	87 W/er	9.6	662
SCN-1	SCN-1	9.9	685
SCZ-8	SCZ-8	9.5	837
Schott A	G018-281	4.6	927
Schott B	G018-305	13.0	908
Schott C	G018-337	8.1	662
Schott D	G018-311	9.8	770
Schott E	GM31107	10.0	649

Source: Data taken from manufacturers' product literature.

Initially, a single glass is mixed with LSM in the range 0–50 wt% glass. These mixtures are characterized for conductivity, mechanical properties, and reaction between the LSM and glass. The optimal mixture ratio is chosen, and then several commercially available glasses are mixed with LSM at this fixed mixture ratio to explore the effect of glass composition. Mixtures with SSC as the conductor composition are also assessed, because the conductivity of SSC is roughly an order of magnitude higher than that of LSM [2]. Finally, the most promising glass/CCM mixtures are applied to MCO-coated 441 steel coupons and tested for area-specific resistance (ASR).

3. Experimental methods

3.1. Materials

Powders of LSM ($La_{0.65}Sr_{0.15}MnO_3$) and SSC ($Sm_{0.5}Sr_{0.5}CoO_3$) were purchased from Praxair. Glass powders were purchased from Spruce Pine Batch (SPG), SEM-COM (SCN-1 and SCZ-8) and Schott (A: G018-281, B: G018-305, C: G018-337, D: G018-311, E: GM31107). Thermal properties of each glass are reported in Table 1.

3.2. Conductivity

Mixed glass and cathode powder of each composition was ball-milled with binder (polyvinyl butyral, dibutyl phthalate, and Menhaden fish oil) in IPA, dried, sieved, and pressed into bars. The bars were sintered at 1000 °C for 1 h in air. The dimensions of the sintered bars were about 1.5 × 3 × 40 mm. Pt mesh current leads were applied to the ends of the bars with Pt paste, and Pt wire voltage leads were wrapped around the bar at 0.5 cm to either side

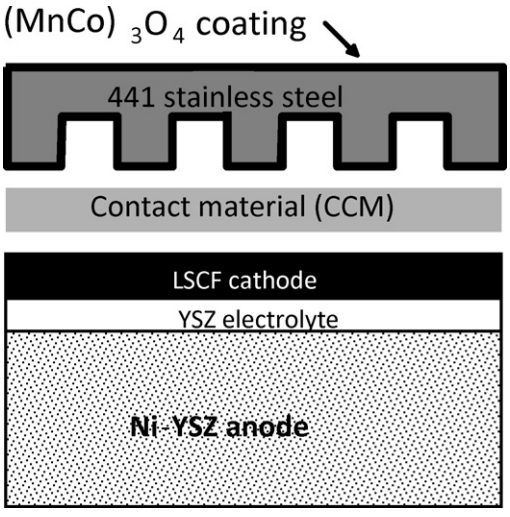

Fig. 1. Schematic representation of CCM placed between SOFC cell and coated stainless steel interconnect.

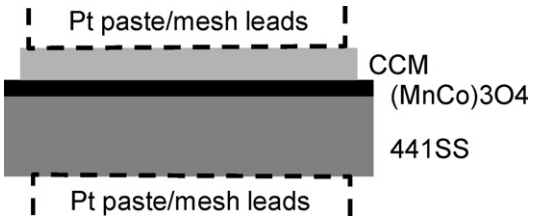

Fig. 2. Schematic representation of ASR specimen geometries. (a) CCM/MCO-441 and (b) CCM/LSCF.

of the centerline. Four-probe DC resistance measurements were taken at 650–900 °C in air using a potentiostat-galvanostat (Biologic VMP-3).

3.3. XRD and SEM

XRD (Philips X'Pert) was used to check reaction between glass and LSM or SSC. XRD traces for pure LSM and SSC powder were compared to those for pellets of mixed cathode and glass (as above) after sintering at 1000 °C for 1 h in air.

Fracture surfaces of the sintered mixtures were imaged with SEM and EDS (Hitachi S4300SE/N).

3.4. CTE

Small pellets of powder and binder were sintered to 1000 °C for 1 h in air (as above). The sintered pellets were then loaded into a contacting dilatometer (Linseis L75) for CTE measurement from 300 to 900 °C in air with a heating rate of 3 °C min^{-1}.

3.5. Dilatometry

Small pellets of powder and binder (as above) were sintered in a contacting dilatometer (Linseis L75) in air from room temperature to 1000–1100 °C (depending on powder melting temperature). The

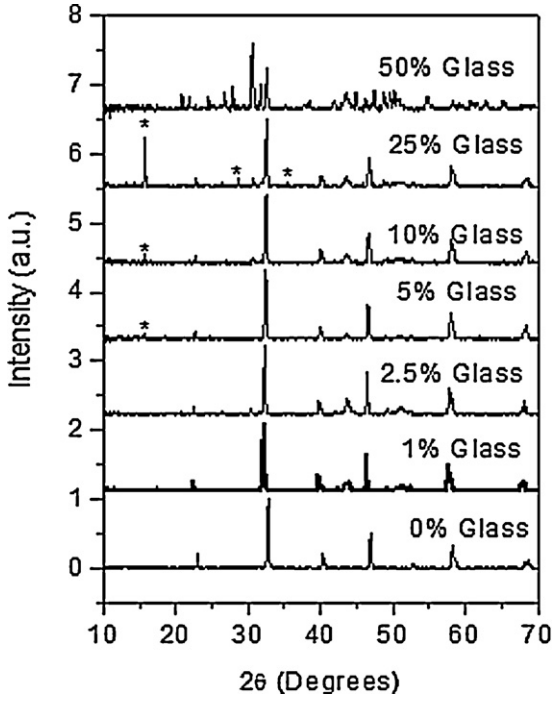

Fig. 3. XRD traces for sintered LSM/SPG mixtures. Weight percent loadings of SPG glass are indicated in the figure.

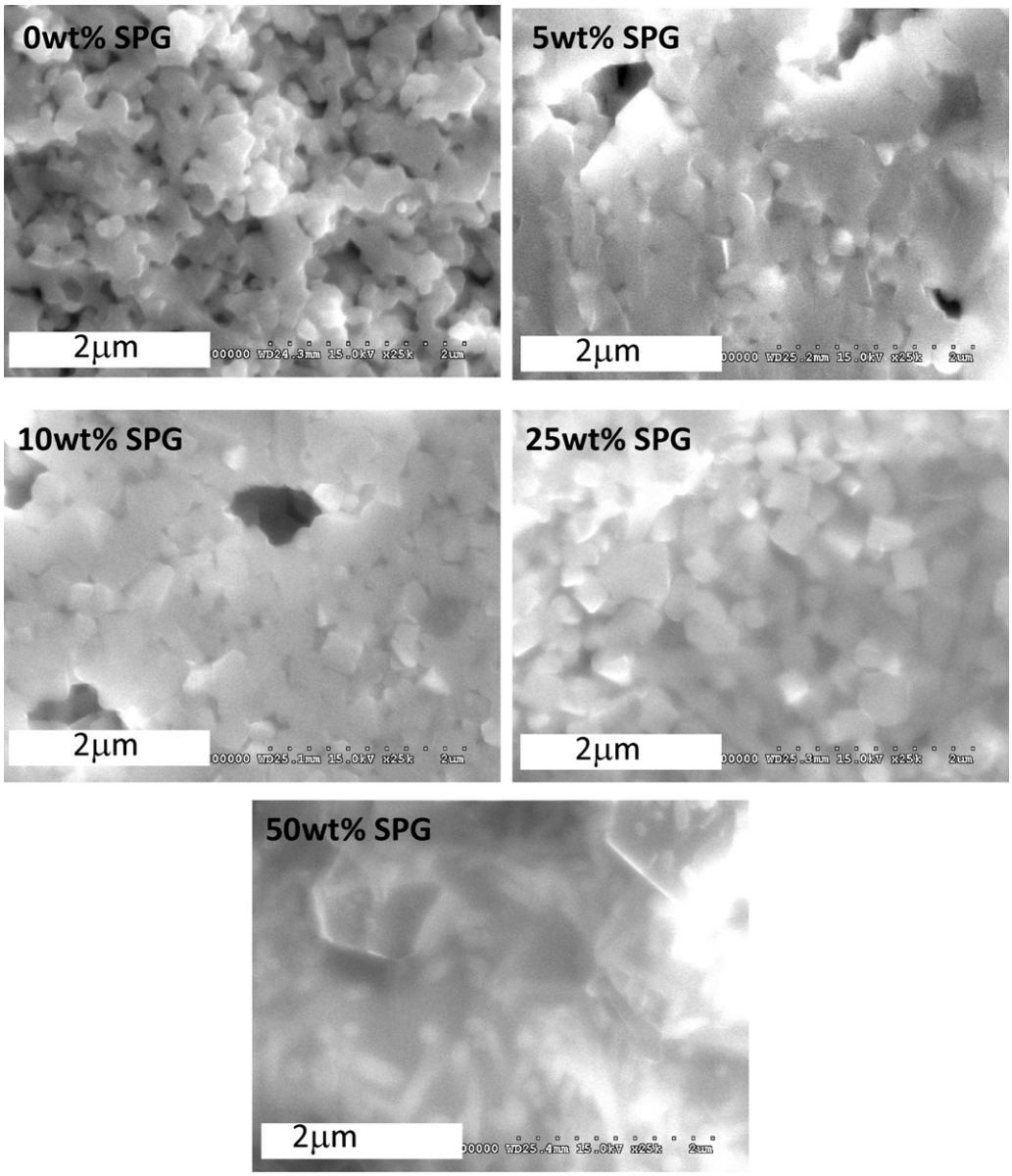

Fig. 4. SEM images of the fracture surface of various sintered LSM/SPG mixtures. Weight percent loadings of SPG glass are indicated in the figure.

heating rate was 3 °C min^{-1}, followed by a 2 h hold at the maximum temperature. The data presented below in Section 4.2 have been adjusted to remove binder burnout, such that the zero-point occurs at 600 °C (above binder features, and below sintering features).

3.6. ASR measurements

Specimens for ASR measurements were prepared according to the geometry in Fig. 2. Various CCM inks were prepared by mixing the powders with Ferro B75717 printing vehicle using a planetary mixer (Thinky). 441 stainless steel coupons were coated with MCO by screenprinting at Pacific Northwest National Laboratory (PNNL). CCM layers were then screenprinted onto the MCO layer, dried under a heatlamp and sintered in air at 1000 °C for 1 h. Pt paste (Heraeus CL11-5349) and Pt mesh (Alfa Aesar 10283) were applied as current collectors on the CCM layers, and sintered at 800 °C. Pt mesh was spot-welded to the 441 coupon. The ASR specimens were then subjected to 500 mA current for 200 h at 800 °C in air. DC current was applied in a 4-probe configuration using a Biologic VMP3 potentiostat.

3.7. Mechanical analysis

Vickers hardness was determined using a Vickers indentation tip loaded with 1 kg dead weight, using a Micromet microhardness tester (Buehler). Interfacial adhesion was assessed using an epoxy-stud pull tester (Quad Group Sebastian V). Glass/CCM inks were printed and sintered onto LSCF and MCO-441 coupons as above.

4. Results and discussion

4.1. LSM–SPG mixtures

Mixtures of LSM and SPG glass ranging from pure LSM to 50 wt% glass were prepared to assess the general behavior of a well-studied SOFC cathode composition upon addition of glass. Fig. 3 shows XRD

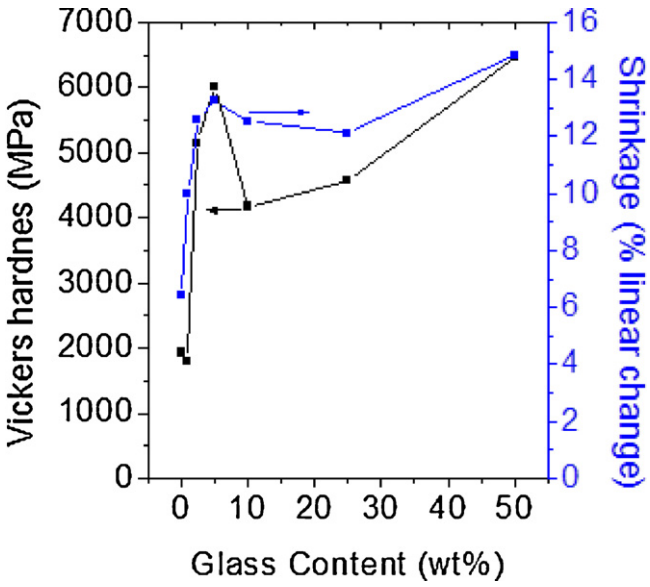

Fig. 5. Vickers hardness and shrinkage-upon-sintering for various LSM/SPG mixtures.

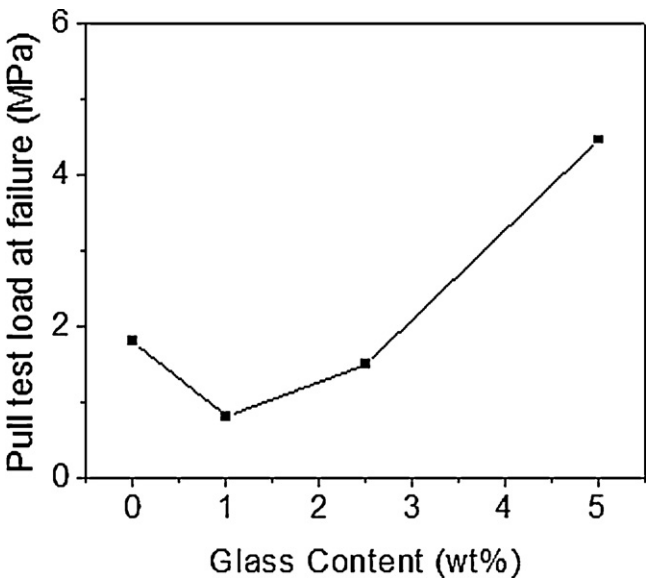

Fig. 6. Adhesion of LSM/SPG mixtures to MCO-coated 441 stainless steel as a function of glass content.

traces for various mixtures after sintering at 1000 °C. Only peaks corresponding to pure LSM are observed for 0–2.5 wt% glass. A small peak arising from a new phase is observed at 5 wt% loading, and the height of this peak increases with addition of glass up to 25 wt%. The XRD trace for pure glass (not shown) does not contain any peaks, as expected for an amorphous material. Therefore, the new peak is attributed to a reaction product of LSM and glass. At 50 wt% glass loading, nearly all of the LSM is consumed by reaction, and many peaks assigned to reaction products are observed.

The fracture surfaces of these same mixtures are shown in Fig. 4. Pure LSM is minimally sintered after firing to 1000 °C, and the morphology is characterized by rough particles with many small pores homogeneously dispersed throughout. The morphology changes dramatically upon addition of 5 wt% glass: the particles are well sintered and although a few large pores are visible, most of the fine porosity is removed. Similar morphology is observed for 10 wt% glass. At 25 wt% glass addition the particles become faceted, suggesting grain growth. At 50 wt% glass, the original LSM particles are not observed; complete modification of the morphology has occurred, yielding needle-shaped crystals in a dense surrounding matrix. This is consistent with the consumption of LSM upon addition of 50 wt% glass observed with XRD above.

Figs. 5–7 show physical, mechanical, and electrical properties of the LSM–SPG mixtures. Pellets of LSM–SPG mixtures were sintered at 1000 °C. Fig. 5 shows the shrinkage upon sintering and Vickers indentation hardness. The indentation hardness is a measure of a material's resistance to plastic deformation. For these minimally sintered samples, we expect the hardness to scale with extent-of-sintering and therefore use it as an indication of mechanical integrity generated by particle-to-particle bonding within the porous microstructure. Both shrinkage and hardness increase dramatically upon addition of up to 5 wt% glass, and then plateau or even decrease with higher glass content. Adhesion of LSM–SPG mixtures to MCO-coated 441 steel substrate was determined by stud pull test, and shown in Fig. 6. Addition of 5 wt% glass is required before a significant improvement is adhesion is observed. Fig. 7 shows the effect of glass addition on conductivity. In all cases, the conductivity is not a very strong function of temperature. At low glass loading (1 wt% and 2.5 wt%) the conductivity is not significantly compromised. At 5 wt% glass loading, the conductivity is reduced by about an order of magnitude. These observations clearly suggest a trade-off between improved mechanical properties and decreased conductivity upon addition of SPG glass to LSM. At a loading level of 5 wt%, these effects are clearly observed, and higher loading gives rise to significantly reduced conductivity without much gain in mechanical properties. We therefore selected 5 wt% glass addition as the loading level for comparison of a variety of glass compositions as described below in Section 4.2.

4.2. Screening various glass compositions

A variety of glass compositions were selected as candidates to improve the mechanical properties of the cathode contact material. The selected glasses are marketed as SOFC sealing glasses, and are all silicate-based. They display a wide range of CTE and softening point, as shown in Table 1. Mixtures of LSM with 5 wt% of each glass were prepared and screened for shrinkage, conductivity, hardness, and chemical reaction. The results are summarized in Table 2 and discussed in more detail below. SSC was also chosen as a candidate CCM because it has a much higher conductivity than

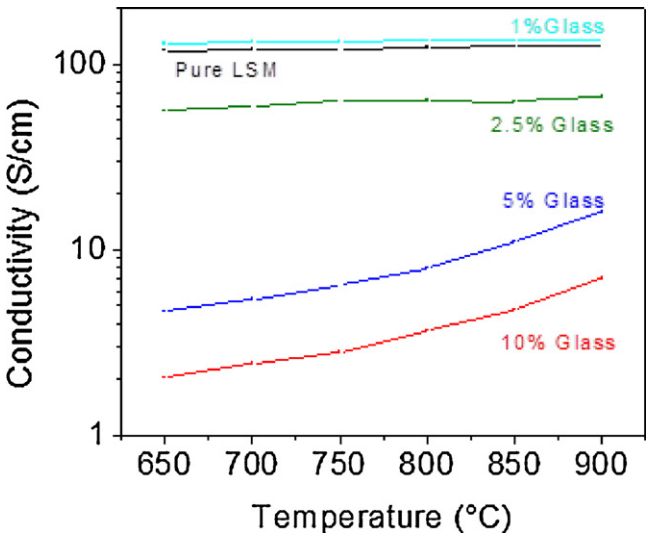

Fig. 7. Temperature-dependence of the conductivity for various LSM/SPG mixtures.

Table 2
Summary of screening results for various CCM/glass mixtures.

CCM	Glass	Shrinkage at 1000 °C (%)	Vickers hardness (MPa)	Stud pull test on LSCF (MPa)	Stud pull test on 441 MCO (MPa)
LSM	None	6.4	1931	3.9	1.8
LSM	SPG	13.3	6006		
LSM	SCZ-8	8.1	2839	5.3	2.9
LSM	SCN-1	11.1	5047		
LSM	Schott A	12.7	4727		
LSM	Schott B	14.4	5401		
LSM	Schott C	13.3	3929		
LSM	Schott D	14.1	5592		
LSM	Schott E	13.7	5401	4.8	3.9

LSM [5–7]. A limited number of glass candidates were mixed with SSC. Of the Schott glass candidates, E provided the best conductivity when mixed with LSM, so only this composition was mixed with SSC.

Pellets of all the compositions were sintered to 1000 °C, and subjected to Vickers indentation. For LSM, all glasses except for SCZ-8 resulted in significant improvement in shrinkage and hardness. For SSC, addition of SPG and SCN-1 resulted in reduced shrinkage and hardness. Addition of SCZ-8 and Schott E to SSC had minimal effect on shrinkage and moderately improved hardness. XRD was used to determine if reaction between the glass and CCM had occurred during firing at 1000 °C. The results are summarized in Table 2, and Fig. 8 shows representative XRD traces. For the case of LSM/Schott D, a single small peak assigned to reaction product is observed, suggesting minimal reaction. For the case of LSM/SCN-1, several larger peaks assigned to reaction products are observed, suggesting significant reaction.

Fig. 9 shows the electronic conductivity for all mixtures after sintering at 1000 °C. In all cases, addition of glass reduces the conductivity. Possible mechanisms include reaction with the CCM, or migration of glass into the electronic percolation path between CCM particles. The general trends with temperature are consistent with those for pure LSM or SSC, suggesting that addition of glass does not significantly alter the mechanism of electronic conduction. For both LSM and SSC, addition of SCZ-8 and Schott E glasses reduced the conductivity less than 50%. SPG addition to SSC also fulfilled this criterion. Addition of other glass compositions reduced the conductivity significantly more.

Based on the screening properties summarized in Table 2, we chose SCZ-8 and Schott E as the most promising glass compositions for further testing and development. Both of these imparted improved hardness without causing significant reaction, nor reducing the conductivity by more than 50%.

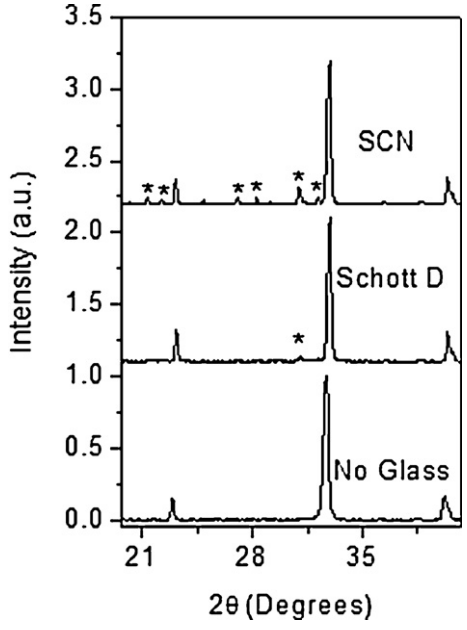

Fig. 8. XRD traces for sintered LSM/Glass mixtures. Glass loading was 5 wt%.

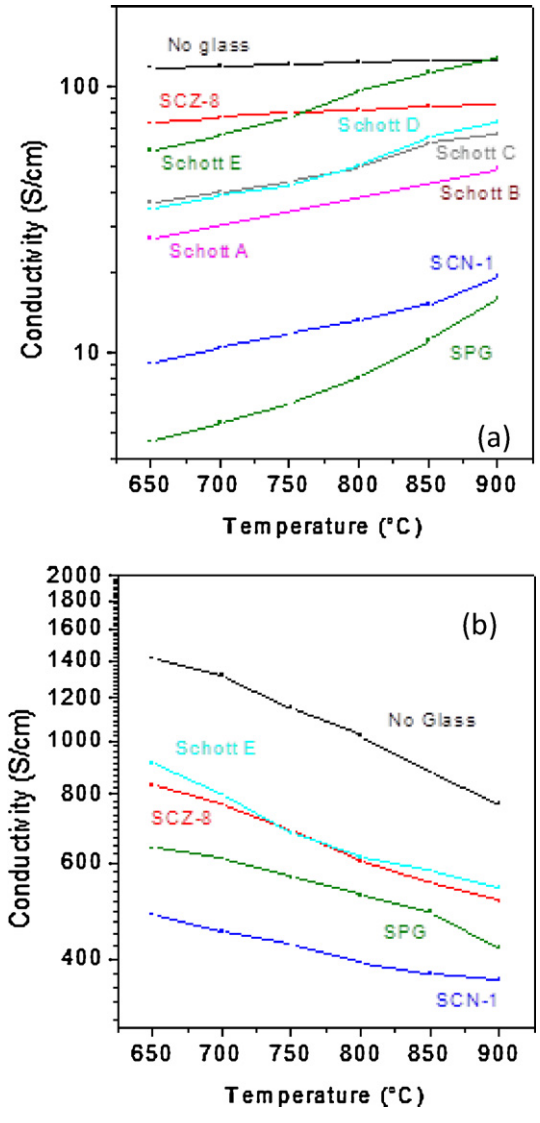

Fig. 9. Conductivity for various sintered CCM/glass (5 wt% glass) mixtures. (a) LSM/glass and (b) SSC/glass.

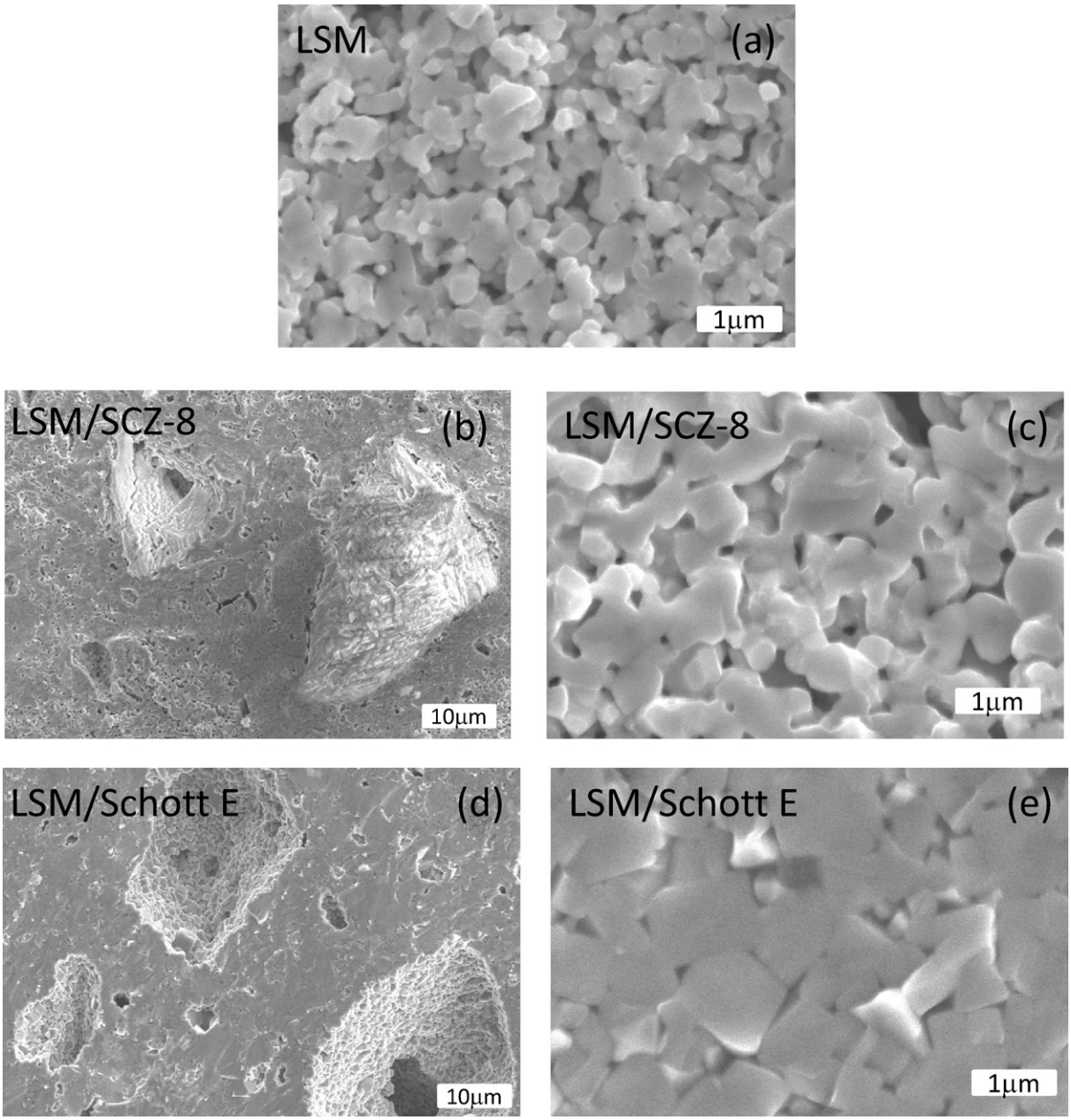

Fig. 10. SEM images of the fracture section of (a) LSM, (b and c) LSM/SCZ-8, and (d and e) LSM/Schott E. Glass loading was 5 wt%.

4.3. Properties of most promising compositions

Fracture surfaces of LSM/glass mixtures after sintering at 1000 °C are shown in Fig. 10. The microstructure of pure LSM is characterized by submicrometer individual particles, with significant porosity uniformly dispersed throughout. This is typical for a minimally sintered ceramic powder compact. The microstructure of the LSM/SCZ-8 mixture is similar, although the particles are larger and noticeably more sintered. In the low-magnification image, it is clear that much of the glass remains intact after sintering. Two sharp-edged 20–30 μm particles of glass, surrounded by LSM particles are seen in the image. This particle size corresponds with that of the as-received glass powder. The microstructure for LSM/Schott E is quite different. Similar sharp-edged features are observed in the low-magnification image, however they are empty. This suggests the glass has moved from its original location into the surrounding LSM matrix, presumably by capillary action. The microstructure of the LSM particles away from the glass particles is significantly denser and more completely sintered than for pure LSM, again suggesting significant interaction of the glass with LSM throughout the whole mixture. Note that the softening temperature of Schott E is almost 200 °C lower than that of SCZ-8 (Table 1), consistent with the observed mobility of Schott E during sintering. The same general features were observed for SSC/SCZ-8 and SSC/Schott E mixtures, although the images are not shown for space considerations.

The impact of glass addition on the sintering behavior of LSM and SSC is shown in Fig. 11. In both cases, addition of SCZ-8 moderately increases sintering and Schott E dramatically increases sintering. This is consistent with the microstructural observations above, as well as with the large improvement in Vickers hardness upon addition of Schott E glass. The large change in sintering behavior upon

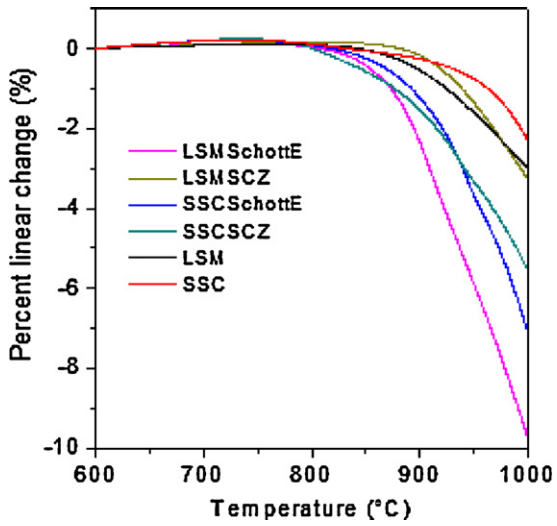

Fig. 11. Sintering behavior of various CCM/glass mixtures. Glass loading was 5 wt%.

addition of only 5 wt% (2.9 v%) Schott E to either LSM or SSC suggests the glass is acting as a sintering aid. If the glass were only melting and filling some of the pore space of the ceramic matrix, such a large shrinkage would not be expected. Clearly, the composition of the glass has a strong effect on its effectiveness as a sintering aid. The CTE of pre-sintered pellets of CCM/glass mixtures is shown in Fig. 12. For both LSM and SSC, addition of glass reduces the CTE, improving the CTE match to other cell materials including YSZ.

Shrinkage and Vickers hardness were expedient screening parameters for down-selecting the most promising glass candidates (Section 4.2), but those tests do not directly assess whether the addition of glass to the CCM improves adhesion to the LSCF cathode or MCO interconnect coating. Therefore, pull tests were performed with the most promising CCM/glass mixtures. The CCM/glass mixtures were screen-printed and sintered onto MCO-coated 441 steel coupons and porous LSCF layers (presintered on dense LSCF coupons). Epoxy-coated studs were used to assess adhesion of the CCM/glass layer to the substrates. In all cases, failure occurred within the CCM/glass layer or at the interface to the substrate (as opposed to within the substrate). The results are reported in Table 2. For LSM, addition of both SCZ-8 and Schott E improved adhesion to both LSCF and MCO. For SSC, adhesion to LSCF was

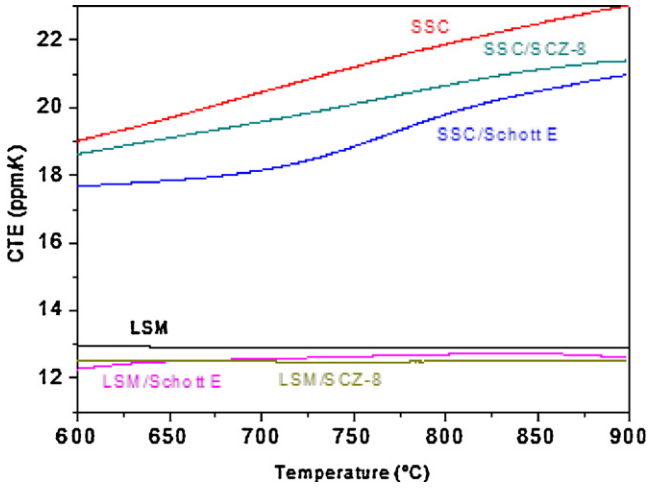

Fig. 12. Temperature-dependence of the CTE for various CCM/glass mixtures. Glass loading was 5 wt%.

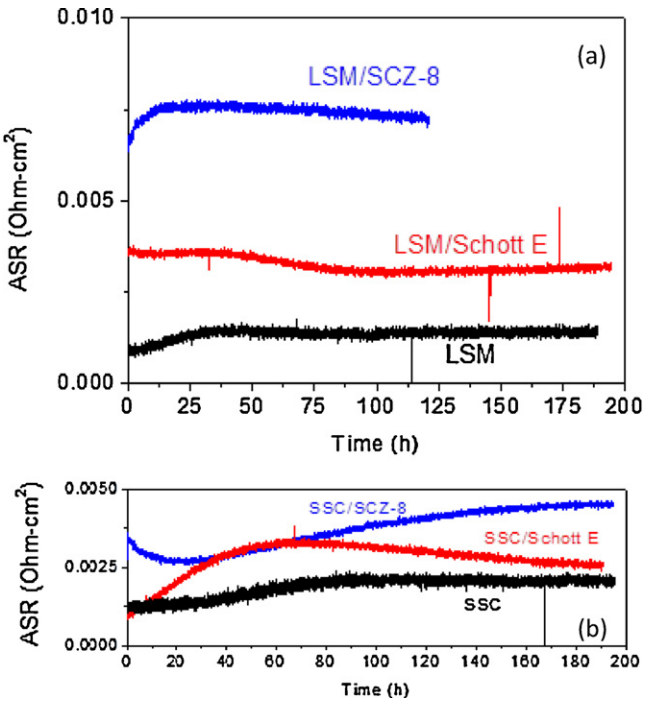

Fig. 13. ASR at 800 °C in air for (a) LSM/glass and (b) SSC/glass mixtures on MCO-coated 441 stainless steel substrates. Glass loading was 5 wt%.

improved, but both glasses reduced adhesion to MCO. It is not clear why this is the case, although we note that the large CTE difference between SSC (~21 ppm K^{-1}) and 441 stainless steel (~13 ppm K^{-1}) may be a factor. These pull test results clearly indicate that addition of glass to the CCM can be an effective strategy to improve the adhesion to neighboring materials at room temperature. Future work will determine if the improved adhesion persists at the 800 °C operating temperature.

4.4. ASR results for most promising compositions

The most promising CCM/glass combinations (and pure CCMs as baseline) were applied to MCO-coated 441 stainless steel interconnect coupons and assessed for area-specific resistance (ASR). The specimens were subjected to 0.5 mA cm^{-2} at 800 °C for 125 h or longer, and the results are shown in Fig. 13. Both pure LSM and SSC displayed a relatively low initial ASR, which roughly doubled over the first 75 h of testing and then became stable. Addition of both glasses to LSM caused an increase in initial ASR, but did not adversely affect stability after the initial 25 h of transient behavior. The increase in ASR upon addition of glass is larger than would be predicted by the increase in conductivity for the bulk materials (Fig. 9 and Table 2). It is unclear why this is the case. Reaction of the glass with the substrate is ruled out by the EDAX analysis below. We speculate that the discrepancy arises from differenced in the microstructure of the bulk and thin layer CCM/glass mixtures for the following two reasons. The bulk material shrinks significantly upon sintering, whereas the thin layer applied to MCO-441 substrate is constrained during sintering. Also, the bulk material was mixed by ball mill so relatively large glass particles remain intact. In contrast, the thin layer ink was mixed in a planetary mill, so reduction of the glass particle size and therefore improved dispersion of the glass throughout the mixture is expected. For SSC, addition of glass caused a relatively small increase in initial ASR, but the ASR was somewhat less stable than for pure SSC or the LSM/glass combinations. Note that even the highest ASR recorded, for LSM/SCZ-8, is

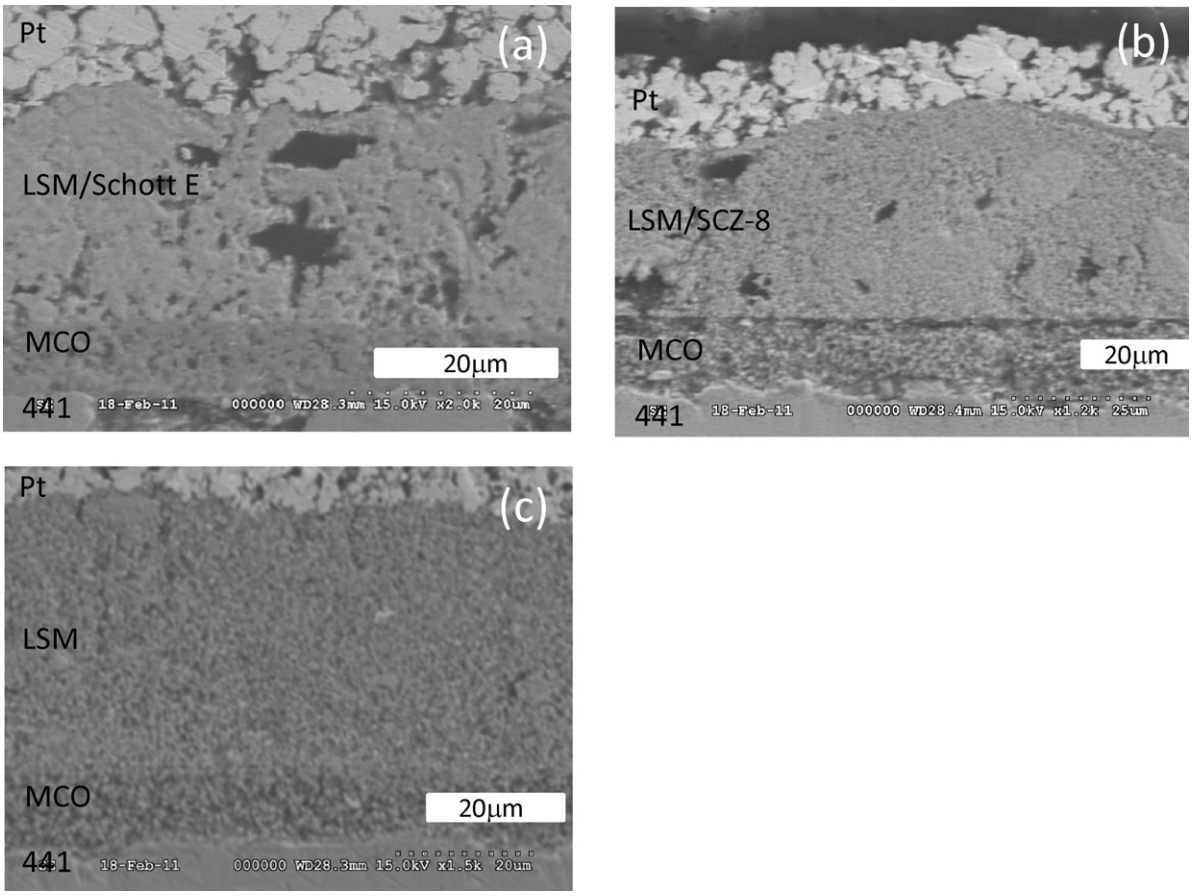

Fig. 14. Cross-section SEM images of LSM/glass and LSM layers on MCO-coated 441 stainless steel substrates after ASR testing.

deemed acceptable because it is much lower than the ASR expected for an operating SOFC.

After ASR testing, the specimens were cross-sectioned and analyzed with SEM/EDAX. Representative results are shown in Figs. 14 and 15. In all cases, good bonding and a crisp transition at the CCM/MCO interface is observed. For the layers with glass, small voids are visible, presumably arising from glass particles as observed above in Fig. 10. The cross-sections of specimens with SSC (not shown) were similar. EDAX analysis was used to determine the extent of interdiffusion between the CCM/glass and MCO layers. In all cases, no significant interdiffusion was observed. The results for LSM/SCZ-8 (the composition showing the highest ASR) are shown in Fig. 15. No interdiffusion is observed. Note that the EDAX peaks for Si and Sr overlap, but neither is observed in the MCO layer.

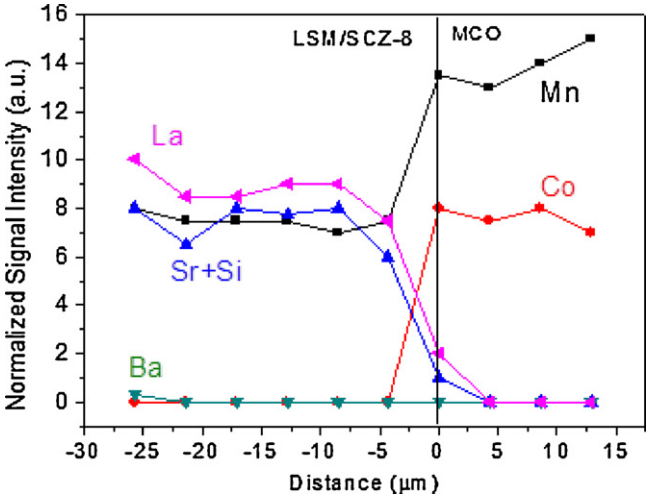

Fig. 15. EDAX linescan across the interface between LSM/SCZ-8 and MCO-coated 441 stainless steel.

5. Conclusions

The feasibility of adding glass to conventional CCM materials in order to improve bonding has been assessed. The composition of the glass plays a significant role in the quality of the resulting composite. Many glasses reacted with the CCM or reduced the conductivity of the CCM/glass composite to an unacceptably low level. The glasses SCZ-8 and Schott E reduced the conductivity minimally, and so were pursued further. Addition of both glasses to LSM improved adhesion to LSCF and MCO-441 substrates, resulting in 4.8 and 3.9 MPa respectively. Addition of both glasses to SSC improved adhesion to LSCF substrate, but not to MCO-441. The ASR of CCM/glass composite layers was moderately higher than that of pure CCM materials, falling in the range 2.5–7.5 mOhm cm^2. Based on these results, we conclude that addition of glass to the CCM is an effective strategy to improve bonding and mechanical properties of the resulting CCM/glass composite, without sacrificing acceptable conductivity. Addition of Schott E glass to LSM was a particularly satisfying example; adhesion strength was significantly improved, while maintaining a low and stable ASR. Future work will determine if the improvement in bonding persists at the SOFC operating temperature, and whether the addition of glass has

unforeseen consequences on the cathode performance of operating SOFC cells.

Acknowledgements

This work was supported by the U.S. Department of Energy, National Energy Technology Laboratory and in part by the U.S. Department of Energy under Contract No. DE-AC02-05CH11231. The authors thank Program Manager Joseph Stoffa, and Jeffry Stevenson and Ryan Scott at Pacific Northwest National Laboratory for MCO deposition.

References

[1] S. Sugita, Y. Yoshida, H. Orui, K. Nozawa, M. u Arakawa, H. Arai, J. Power Sources 185 (2008) 932–936.
[2] M.C. Tucker, L. Cheng, L.C. DeJonghe, J. Power Sources, in press, doi:10.1016/j.jpowsour.2011.06.044.
[3] S. Simner, M. Anderson, J. Bonnett, J. Stevenson, Solid State Ionics 175 (2004) 79–81.
[4] B.P. McCarthy, L.R. Pederson, Y.S. Chou, X.-D. Zhou, W.A. Surdoval, L.C Wilson, J. Power Sources 180 (2008) 294–300.
[5] J. Fergus, J. Power Sources 147 (2005) 46–57.
[6] M.K. Mahapatra, K. Lu, Mater. Sci. Eng. R 67 (2010) 65–85.
[7] S. Yang, T. He, Q. He, J. Alloys Compounds 450 (2008) 400–404.